International Journal of Recent Research and Review, Vol. XIII, Issue 3, September 2020
ISSN 2277 – 8322

Design and Development of Hybrid Electrical Vehicle Using BLDC Motor

Sonali Vidhate[1],Tushar Tambe[2],Pawan Tapre[3],Amit Solanki[4]
SND College of Engineering and Research Centre, Yeola
Email: tushar.tambe05@gmail.com

***Abstract*--- Electric vehicles (EV), including Battery Electric Vehicle (BEV), Hybrid Electric Vehicle (HEV), Plug-in Hybrid Electric Vehicle (PHEV), Fuel Cell Electric Vehicle (FCEV), are becoming more commonplace in the transportation sector in recent times. As the present trend suggests, this mode of transport is likely to replace internal combustion engine (ICE) vehicles in the near future. Each of the main EV components has a number of technologies that are currently in use or can become prominent in the future. EVs can cause significant impacts on the environment, power system, and other related sectors. The present power system could face huge instabilities with enough EV penetration, but with proper management and coordination, EVs can be turned into a major contributor to the successful implementation of the smart grid concept. There are possibilities of immense environmental benefits as well, as the EVs can extensively reduce the greenhouse gas emissions produced by the transportation sector. However, there are some major obstacles for EVs to overcome before totally replacing ICE vehicles. Industrial Motor Drives mainly deals with operations at base speed of motor. Electric Vehicle Motor Drives deals with operations that require sudden start and stop, low speed operations and base speed operations as well. The system should meet the objective of variable speed, variable torque applications like Electric Vehicles (EVs). As per studies, BLDC motor is found to be a suitable motive element for EV application based on its suitable torque speed characteristics. The system needs to implement with a suitable control mechanism that will help to operate the motor in an efficient manner**.

***Keywords* - Electric Vehicle; Energy Sources; Electric Motors; Motor Characteristics**

I. INTRODUCTION

Electric vehicles (EV), including Battery Electric Vehicle (BEV), Hybrid Electric Vehicle (HEV), Plug-in Hybrid Electric Vehicle (PHEV), Fuel Cell Electric Vehicle (FCEV), are becoming more commonplace in the transportation sector in recent times [1,2]. With increase in EVs, the impact of smart charging and fast charging on the power system is explained along with its impact on the battery state of health and degradation is studied [3,4].

Most EVs are sourcing DC voltage. A direct use of DC is preferred as it avoids use of additional converter hardware. The battery performance depends not only on types and design of the batteries, but also on charger characteristics and charging infrastructure [5,6]. Combining high-energy-density batteries and high-power-density ultra-capacitors in fuel cell hybrid electric vehicles (FCHEVs) results in a high-performance, highly efficient, low-size, and light system. Often, the battery is rated with respect to its energy requirement to reduce its volume and mass [7,8].

The operations and circumstances faced by the motor drive system for EV includes:

- Sudden Start/Stop capacity with damage
- High torque generating capacity
- High acceleration
- High power intensity
- High torque when operating at slow speeds with a high efficiency (To run on any terrain and in harsh environments)
- High Efficiency with respect to the regenerative braking capacity (for battery charging)

All of the electrical motors that do not require an electrical connection (made with brushes) between stationary and rotating parts can be considered as brushless permanent magnet (PM) machines which can be categorized based on the PMs mounting and the back-EMF shape [13,14]. The PMs can be surface mounted on the rotor (SMPM) or installed inside of the rotor (IPM), and the back-EMF shape can either be sinusoidal or trapezoidal. According to the back-EMF shape, PM AC synchronous motors (PMAC or PMSM) have sinusoidal back-EMF and Brushless DC motors (BLDC or BPM) have trapezoidal back-EMF. A PMAC motor is typically excited by a three-phase sinusoidal current, and a BLDC motor is usually powered by a set of currents having a quasi-square waveform [21,22].

The BLDC motor provides an attractive candidate for sensor-less operation because the nature of its excitation inherently offers a low-cost way to extract rotor position information from motor-terminal voltages. In the excitation of a three-phase BLDC motor, except for the phase-commutation periods, only two of the three phase windings are conducting at a time and the no conducting phase carries the back-EMF. There are many categories of sensor-less control strategies [23].

The most popular category is based on back electromotive forces or back-EMFs. Sensing back-EMF of unused phase is the most cost-efficient method to obtain the commutation sequence in star wound motors. Since back-EMF is zero at standstill and proportional to speed, the measured terminal voltage that has large signal-to-noise ratio cannot detect zero crossing at low speeds. That is the reason why in all back-EMF-based sensor-less methods the low-speed performance is limited, and an open-loop starting strategy is required [24].

II. METHODOLOGY

PM motor drives require a rotor position sensor to properly perform phase commutation and/or current control. For PMAC motors, a constant supply of position information is necessary; thus a position sensor with high resolution, such as a shaft encoder or a resolver, is typically used. For BLDC motors, only the knowledge of six phase-commutation instants per electrical cycle is needed; therefore, low-cost Hall-effect sensors are usually used. Also, electromagnetic variable reluctance (VR) sensors or accelerometers have been extensively applied to measure motor position and speed. The reality is that angular motion sensors based on magnetic field sensing principles stand out because of their many inherent advantages and sensing benefits [9,10].

An accelerometer is a electromechanical device that measures acceleration forces, which are related to the freefall effect. Several types are available to detect magnitude and direction of the acceleration as a vector quantity, and can be used to sense position, vibration and shock. The most common design is based on a combination of Newton's law of mass acceleration and Hooke's law of spring action. Then, conceptually, an accelerometer behaves as a damped mass on a spring, which is depicted. When the accelerometer experiences acceleration, the mass is displaced to the point that the spring is able to accelerate the mass at the same rate as the casing [12]. The displacement is then measured to give the acceleration. There is a wide variety of accelerometers depending on the requirements of natural frequency, damping, temperature, size, weight, hysteresis, and so on. Some of these types are piezoelectric, piezo-resistive, variable capacitance, linear variable differential transformers (LVDT), potentio-metric, among many others [11]. The MEMS accelerometer is silicon micro-machined, and therefore, can be easily integrated with the signal processing circuits

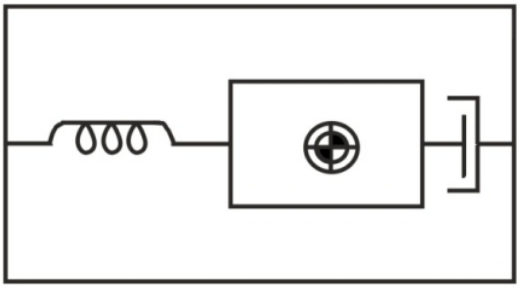

Fig 1 Accelerometer

These kinds of devices are based on Hall-effect theory, which states that if an electric current- carrying conductor is kept in a magnetic field, the magnetic field exerts a transverse force on the moving charge carriers that tends to push them to one side of the conductor. A build-up of charge at the sides of the conductors will balance this magnetic influence producing a measurable voltage between the two sides of the conductor. The presence of this measurable transverse voltage is called the Hall-effect.

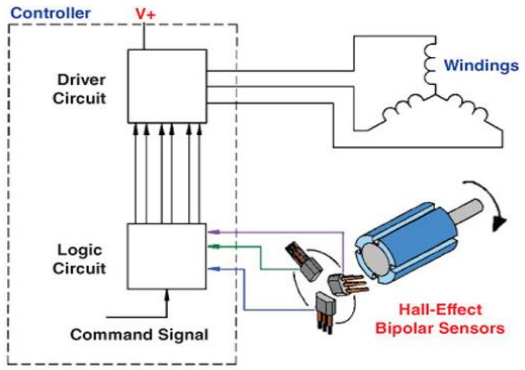

Fig.2 BLDC motor with Hall sensor

Unlike a brushed DC motor, the commutation of a BLDC motor is controlled electronically. To rotate the BLDC motor the stator windings should be energized in a sequence. It is important to know the rotor position in order to understand which winding will be energized following the energizing sequence. Rotor position is sensed using Hall-effect sensors embedded into the stator. Most BLDC motors have three Hall sensors inside the stator on the non-driving end of the motor. Whenever the rotor magnetic poles pass near the Hall sensors they give a high or low signal indicating the N or S pole is passing near the sensors. Based on the combination of these three Hall sensor signals, the exact sequence of commutation can be determined. Figure shows a transverse section of a BLDC motor with a rotor that has alternate N and S permanent magnets. Hall sensors are embedded into the stationary part of the motor [17-18]. Embedding the Hall sensors into the stator is a complex process because any misalignment in these Hall sensors with respect to the rotor magnets will generate an error in determination of the rotor position. To simplify the process of mounting the Hall sensors onto the stator some motors may have the Hall sensor magnets on the rotor, in addition to the main rotor magnets. Therefore, whenever the rotor rotates the Hall sensor magnets give the same effect as the main magnets. The Hall sensors are normally mounted on a printed circuit board and fixed to the enclosure cap on the non-driving end. This enables users to adjust the complete assembly of Hall sensors to align with the rotor magnets in order to achieve the best performance [19 - 20].

This kind of sensor is used to measure position and speed of moving metal components, and is often referred as a passive magnetic sensor because it does not need to be powered. It consists of a permanent magnet, a ferromagnetic pole piece, a pickup coil, and a rotating toothed wheel, as illustrated in figure. This device is basically a permanent magnet with wire wrapped around it. It is usually a simple circuit of only two wires where in most cases polarity is not important, and the physics behind its operation include magnetic induction

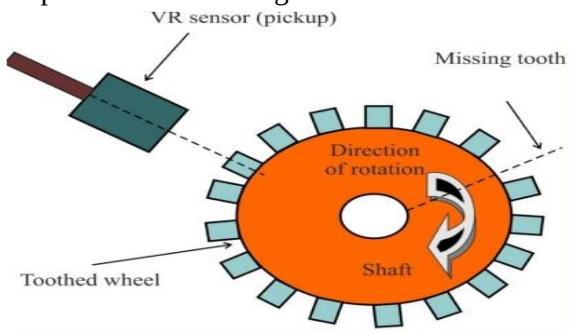

Fig.3 BLDC motor with VR Speed sensor

In principle, the DTC method selects one of the inverter's six voltage vectors and two zero vectors as shown in figure below in order to keep the stator flux and torque within a hysteresis band around the command or reference flux and torque magnitudes. In this model, the ON state of upper limb switches are represented by '1' and the lower limb switches are represented by '0' and the same has been defined [15-16].

The core of DTC consists of hysteresis controllers of torque and flux, switching logic, and motor model as shown in Figure, which shows the basic schematic diagram of classical direct torque control strategy of

induction motor in which there are two different loops corresponding to magnitudes of stator flux and torque provided. The reference values of stator flux and torque are compared with the corresponding actual values calculated by the motor model and the respective errors are obtained.

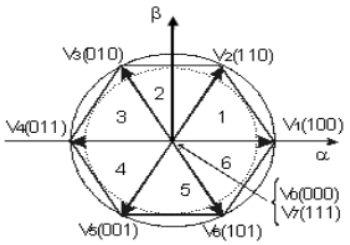

Fig.4 Space vectors and switching states of inverter

The resulting flux error is fed into the two level flux hysteresis and torque error is fed into three level hysteresis controllers. The outputs of torque and flux hysteresis controllers are combined together with the position of stator flux and given as inputs to the switching state selection table I.

Table I

Space vectors and switching states of inverter

Voltage Vectors	Switching States		
	A	B	C
V_0	0	0	0
V_1	1	0	0
V_2	1	1	0
V_3	0	1	0
V_4	0	1	1
V_5	0	0	1
V_6	1	0	1
V_7	1	1	1

With reference to the block diagram of DTC, the stator flux and torque errors tend to be restricted within the hysteresis bands. The flux hysteresis band affects basically the stator current distortion in terms lower order harmonics and torque hysteresis band affects the switching frequency. The DTC requires the stator flux and torque estimations, which are performed by means of two different phase currents and state of the inverter.However, flux and torque estimations can also be performed using mechanical speed and two stator phase currents. The switching logic defines the suitable voltage vector based on torque and flux references. Large and small torque or flux errors are not distinguished. The same vectors are used during start-up, step changes and steady state conditions

III. SIMULINK MOTOR DETAILS

Due to the fact that the software used by commercial e-Bikes is confidential, the software has been designed based on the fundamentals of BLDC motors presented in the introduction of this paper and other studies [2-4]. The commutation scheme used in this design is described in Fig. 5. By analyzing the diagram in Fig. 5, the system of equations (1) has been deduced, through which the control logic has been modeled as a combinational system. The inputs to this combinational system are the Hall position sensors signals and a master PWM, and the outputs are the PWM signals.

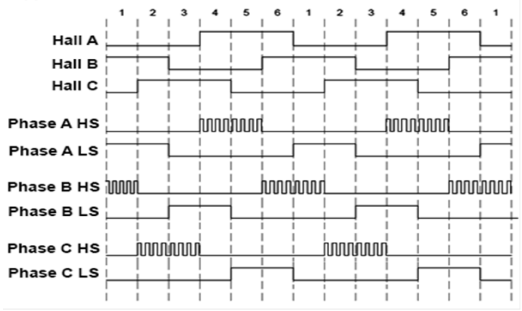

Fig.5 PWM commutation scheme

$$AHS = PWM \cdot (HallA \cdot \overline{HallB});$$
$$BHS = PWM \cdot (HallB \cdot \overline{HallC});$$
$$CHS = PWM \cdot (HallC \cdot \overline{HallA});$$
$$ALS = HallB \cdot \overline{HallA};$$
$$BLS = HallC \cdot \overline{HallB};$$
$$CLS = HallA \cdot \overline{HallC};$$

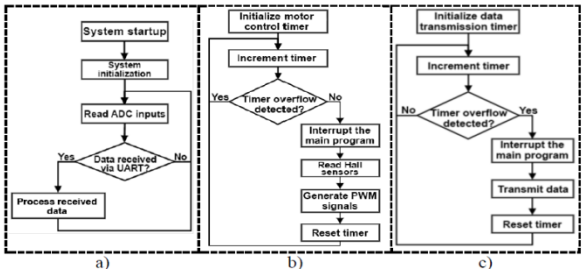

Fig.6 Electronic control unit software flow diagram: a) main program; b) motor control thread; c) data transmission thread

The software presented in the flow diagram, in Fig. 6, is structured in two threads, one for each main function fulfilled. The threads are governed by two separate timers, the motor control thread having the highest priority.

IV. MOTOR SIMULATION DETAILS

The software presented in the flow diagram, in Fig. 5.2, is structured in two threads, one for each main function fulfilled. The threads are governed by two separate timers, the motor control thread having the highest priority. The simulation took into account the commutation table presented in Fig6.The Simulink model is presented in Fig. 7. The results of the simulation are (1) the stator current waveform, (2) rotor speed and (3) electromagnetic torque ripple. These results are shown in the graphs in Fig.8

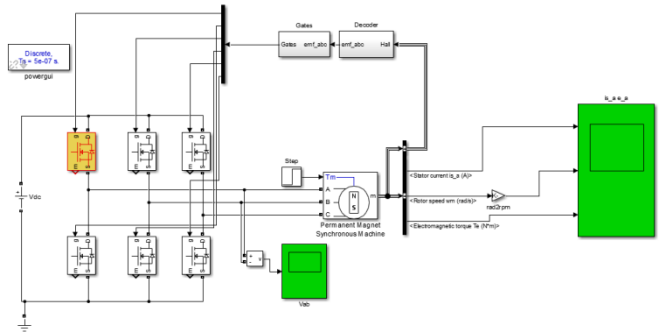

Fig 7 Simulink Motor Model of Proposed System

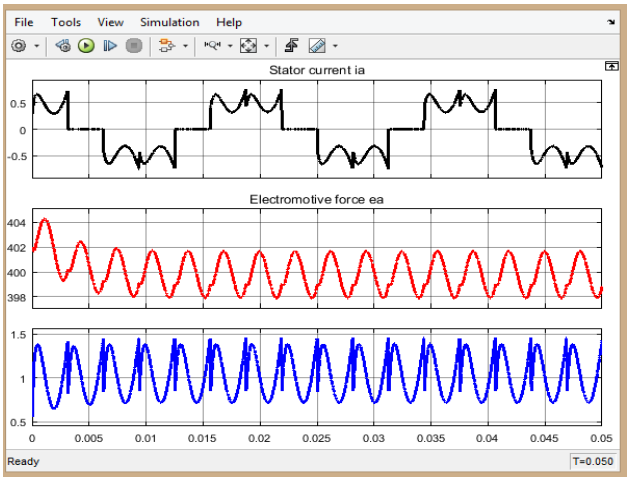

Fig 8Simulation results of Proposed System

V. HEV SYSTEM CONFIGURATION AND LAYOUT

The HEV system selected has a kerb weight of 1325kg and with total range of 870km and electric range of 18km

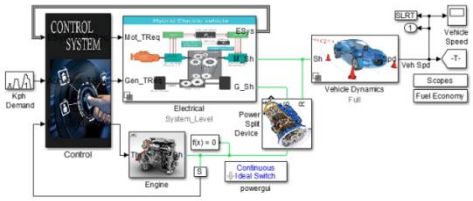

Fig 9 HEV System Level Layout

A. Engine System Requirements

The following requirements apply to the functionality of this module.

ICE

1.	Power	57 kW @5000 RPM
2.	Min Speed	1000 rpm
3.	Max Speed	4500 rpm
4.	Torque	115 Nm @ 4200 RPM

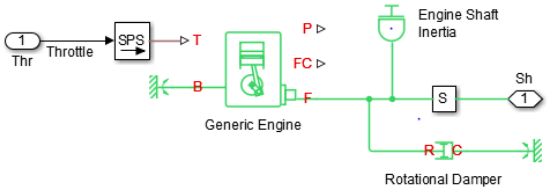

Fig 10 Generic Simscape Engine

B. Fuel Consumption

The following requirements apply to the fuel consumption:

Regular Gas

a.	City	51 MPG
b.	Highway	49 MPG
c.	Combined	50 MPG

A. DRIVE CYCLE 1

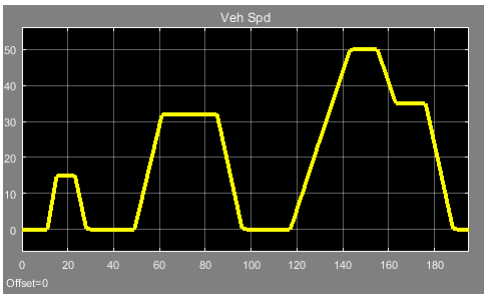

Fig 11 Vehicle Speed

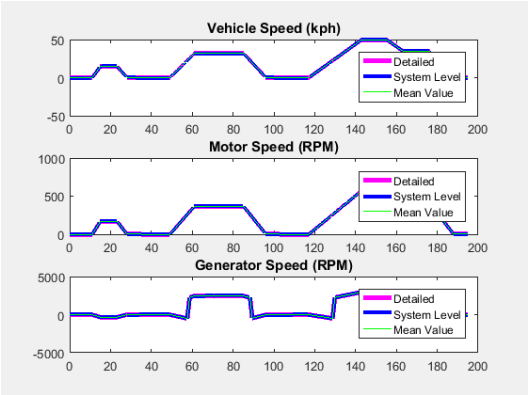

Fig 12 Speeds From Urban Cycle 1

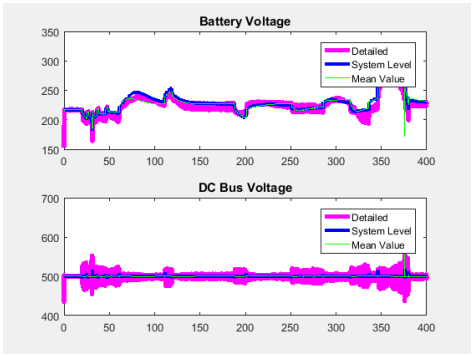

Fig 13 Voltages From Urban Cycle 1

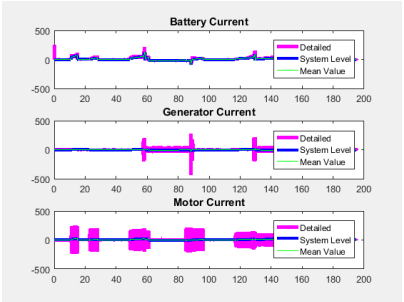

Fig 14 Currents From Urban Cycle 1

B. DRIVE CYCLE 2

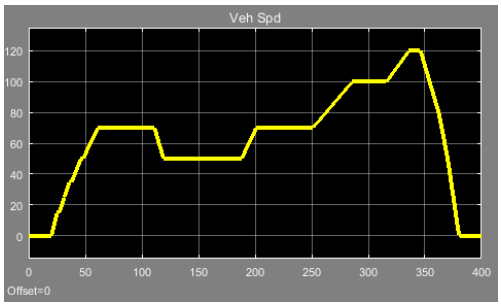

Fig 15Vehicle Speed

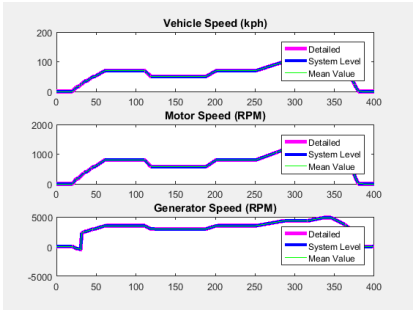

Fig 16Speeds From Urban Cycle 2

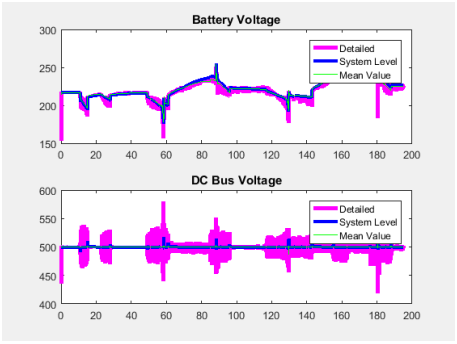

Fig 17 VoltagesFrom Urban Cycle 2

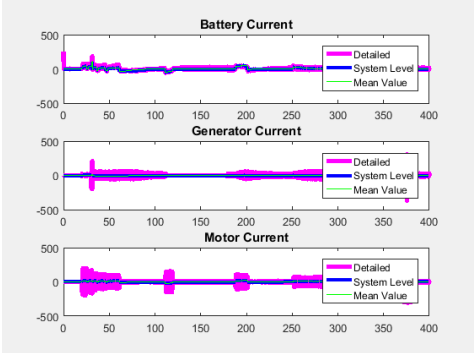

Fig 18 Currents From Urban Cycle

Table II
Simulation Time

Configuration	Elapsed Time	Simulation Time	Sim Time/Elapsed Time
Sys BD VS	4.7654	195	40.9201
Sys BD VS	7.2198	400	55.4033
Sys BD VS	6.7394	400	59.3524

VI.CONCLUSION

A D.C (Direct Current) drive has been used prominently in the E.V's because they provide simple speed control and ideal torque-speed requirements. The ideal torque suits the traction and terrain requirements in an E.V. Their commutator and brushes make them less reliable. So, it is not suitable for a maintenance free function.

With advancements in power electronics, A.C motor drives with IM or PMSM are much more preferred than a D.C drive with advantages of Reliability, Greater Efficiency, Less Maintenance and High Power Density. PMSM offers overall reduction in the weight and volume for a given value of power. Owing to no rotor copper losses, the efficiency is much higher. The reliability is quite high.

But the winner in this selection process for medium size electric vehicle stands out to be BLDC motor drive, which are fed by a rectangular A.C supply. With advantages like elimination of the Brushes, ability to produce a larger Torque than the others at the same values of Current and Voltage, High Power Density and Great Efficiency, P.M Brushless D.C Motor Drive an ideal choice for being used in the Electric Vehicle Propulsion System.

Since BLDC motor has been used widely in automotive, it was tested for simulation profiles and then is integrated in the HEV system model in Simulink.

VII. REFERENCES

[1] Yong, J.Y.; Ramachandaramurthy, V.K.; Tan, K.M.; Mithulananthan, N. A review on the state-of-the-art technologies of electric vehicle, its impacts and prospects. Renew. Sustain. Energy Rev. 2015, 49, 365–385.

[2] Camacho, O.M.F.; Nørgård, P.B.; Rao, N.; Mihet-Popa, L. Electrical Vehicle Batteries Testing in a Distribution Network using Sustainable Energy. IEEE Trans. Smart Grid 2014, 5, 1033–1042.

[3] Camacho, O.M.F.; Mihet-Popa, L. Fast Charging and Smart Charging Tests for Electric Vehicles Batteries using Renewable Energy. Oil Gas Sci. Technol. 2016, 71, 13–25.

[4] Marchesoni, M.; Vacca, C. New DC–DC converter for energy storage system interfacing in fuel cell hybrid electric vehicles. IEEE Trans. Power Electron. 2007, 22, 301–308.

[5] Schaltz, E.; Khaligh, A.; Rasmussen, P.O. Influence of battery/ultracapacitor energy-storage sizing on battery lifetime in a fuel cell hybrid electric vehicle. IEEE Trans. Veh. Technol. 2009, 58, 3882–3891.

[6] Kramer, B.; Chakraborty, S.; Kroposki, B. A review of plug-in vehicles and vehicle-to-grid capability. In Proceedings of the 34th IEEE Industrial Electronics Annual Conference, Orlando, FL, USA, 10–13 November 2008; pp. 2278–2283.

[7] Gao, Y.; Ehsani, M. Design and control methodology of plug-in hybrid electric vehicles. IEEE Trans. Ind. Electron. 2010, 57, 633–640.

[8] EG&G Technical Services, Inc. The Fuel Cell Handbook, 6th ed.; U.S. Department of Energy: Morgantown, WV, USA, 2002.

[9] Miller, J.F.; Webster, C.E.; Tummillo, A.F.; DeLuca, W.H. Testing and evaluation of batteries for a fuel cell powered hybrid bus. In Proceedings of the Energy Conversion Engineering Conference, Honolulu, HI, USA, 27 July–1 August 1997; Volume 2, pp. 894–898.

[10] Rodatz, P.; Garcia, O.; Guzzella, L.; Büchi, F.; Bärtschi, M.; Tsukada, A.; Dietrich, P.; Kötz, R.; Scherer, G.; Wokaun, A. Performance and operational characteristics of a hybrid vehicle powered by fuel cells and supercapacitors. In Proceedings of the SAE 2003 World Congress and Exhibition, Detroit, MI, USA, 3 March 2003; Volume 112, pp. 692–703.

[11] Fuad Un-Noor, SanjeevikumarPadmanaban,*, Lucian Mihet-Popa, Mohammad NurunnabiMollah and EklasHossain, “A Comprehensive Study of Key Electric Vehicle (EV) Components, Technologies, Challenges, Impacts, and Future Direction of Development”, Energies 2017, 10, 1217; doi:10.3390/en10081217

[12] Camacho, O.M.F.; Nørgård, P.B.; Rao, N.; Mihet-Popa, L. Electrical Vehicle Batteries Testing in a Distribution Network using Sustainable Energy. IEEE Trans. Smart Grid 2014, 5, 1033–1042.

[13] Camacho, O.M.F.; Mihet-Popa, L. Fast Charging and Smart Charging Tests for Electric Vehicle Batteries using Renewable Energy, Oil Gas Sci. Technol. 2016, 71, 13–25.
[14] Chan, C.C. The state of the art of electric and hybrid vehicles, Proc. IEEE 2002, 90, 247–275
[15] SAE International. SAE Electric Vehicle and Plug-in Hybrid Electric Vehicle Conductive Charge Coupler, In SAE Standard J1772; Society of Automotive Engineers (SAE): Warrendale, PA, USA, 2010.
[16] Grunditz, E.A.; Thiringer, T. Performance Analysis of Current BEVs Based on a Comprehensive Review of Specifications, IEEE Trans. Transp. Electr. 2016, 2, 270–289.
[17] Yilmaz, M.; Krein, P.T. "Review of battery charger topologies, charging power levels, and infrastructure for plug-in electric and hybrid vehicles", IEEE Trans. Power Electr. 2013, 28, 2151–2169.
[18] Bayindir K.Ç.; Gözüküçük M.A.; Teke A, "A comprehensive overview of hybrid electric vehicle: Powertrain configurations, powertrain control techniques and electronic control units", Energy Convers. Manag. 2011, 52, 1305–1313.
[19] Imura, I.; Uchida, T.; Hori, Y. Flexibility of contactless power transfer using magnetic resonance coupling to air gap and misalignment for EV. World Electr. Veh. J. 2009, 3, 24–34.
[20] Nakadachi, S.; Mochizuki, S.; Sakaino, S.; Kaneko, Y.; Abe, S.; Yasuda, T. Bidirectional contactless power transfer system expandable from unidirectional system. In Proceedings of the 2013 IEEE Energy Conversion Congress and Exposition, Denver, CO, USA, 15–19 September 2013; pp. 3651–3657.
[21] Gao, Y.; Ehsani, M.; Miller, J.M. Hybrid Electric Vehicle: Overview and State of the Art. In Proceedings of the IEEE International Symposium on Industrial Electronics, Dubrovnik, Croatia, 20–23 June 2005; pp. 307– 316.
[22] Kim, H.; Kum, D. Comprehensive Design Methodology of Input- and Output-Split HybridElectric Vehicles: In Search of Optimal Configuration. IEEE/ASME Trans. Mechatron. 2016, 21, 2912–2923.
[23] Miller, J.M. Hybrid electric vehicle propulsion system architectures of the e-CVT type. IEEE Trans. Power Electron. 2006, 21, 756–767.
[24] Kim, D.; Hwang, S.; Kim, H. Vehicle Stability Enhancement of Four-Wheel-Drive Hybrid Electric Vehicle Using Rear Motor Control. IEEE Trans. Veh. Technol. 2008, 57, 727–735.